



Spectroscopic evaluation of several thulium doped laser materials via Fourier transform time-resolved spectroscopy
by Richard Charles Martoglio

A thesis submitted in partial fulfillment of the requirements for the degree of Master of Science in Chemistry (MONTANA STATE UNIVERSITY Bozeman, Montana August 1997
Montana State University
© Copyright by Richard Charles Martoglio (1997)

Abstract:

A new technique for the analysis of solid-state laser materials named Fourier Transform Time-Resolved Spectroscopy (FT-TRS) has been developed and implemented. FT-TRS has advantages over previous analysis techniques, primarily the time in which complete material characterization can be accomplished. The technique uses interferometric methods to collect sample emission after excitation over a broad spectral range while simultaneously characterizing the emission lifetime. In this way, analysis time is shortened considerably while providing information regarding absorption frequencies, emission frequencies and emission lifetimes which are essential for understanding the kinetics of the many photophysical processes which occur in these materials.

The interferometer used for our FT-TRS experiments can resolve spectral features to 0.25 cm^{-1} over a range of nearly 23,000 cm^{-1} (25,000-2,000 cm^{-1}). Temporal resolution to 20 nsec has been achieved. The implementation of an optically parametric oscillating laser enables material excitation from 23,000-5,500 cm^{-1} .

FT-TRS has been used for the analysis of several different thulium (Tm^{3+}) doped laser materials. The technique has proven to yield results consistent with earlier studies performed using different instrumentation. Emission rise and decay lifetimes for several electronic transitions have been determined. Mathematical fitting methods developed by Inokuti and Hirayama have proven to fit non-exponential emission decay that occurs in these materials. Subsequently, the kinetics which describe the many energy transfer events occurring after excitation have been investigated which has yielded the magnitudes of these radiative and non-radiative energy transfer processes.

**SPECTROSCOPIC EVALUATION OF SEVERAL THULIUM DOPED LASER
MATERIALS VIA FOURIER TRANSFORM TIME-RESOLVED SPECTROSCOPY**

by

Richard Charles Martoglio

A thesis submitted in partial fulfillment
of the requirements for the degree

of

Master of Science

in

Chemistry

**MONTANA STATE UNIVERSITY
Bozeman, Montana**

August 1997

N378
M3672

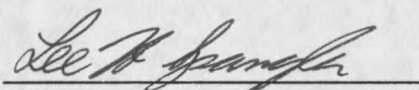
APPROVAL

of a thesis submitted by

Richard Charles Martoglio

This thesis has been read by each member of the thesis committee and has been found to be satisfactory regarding content, English usage, format, citations, bibliographic style, and consistency, and is ready for submission to the College of Graduate Studies.

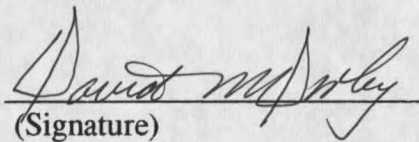
Dr. Lee Spangler


(Signature)

8/15/97
Date

Approved for the Department of Chemistry

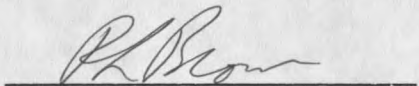
Dr. David Dooley


(Signature)

8/15/97
Date

Approved for the College of Graduate Studies

Dr. Robert Brown


(Signature)

8/15/97
Date

STATEMENT OF PERMISSION TO USE

In presenting this thesis in partial fulfillment of the requirements for a master's degree at Montana State University-Bozeman, I agree that the Library shall make it available to borrowers under rules of the Library.

If I have indicated my intention to copyright this thesis by including a copyright notice page, copying is allowable only for scholarly purposes, consistent with "fair use" as prescribed in the U.S. Copyright Law. Requests for permission for extended quotation from or reproduction of this thesis in whole or in parts may be granted only by the copyright holder.

Signature Richard Charles Mayo

Date 8/15/97

ACKNOWLEDGMENTS

I would like to thank Dr. Lee Spangler for his guidance, instruction, motivation and support while pursuing this degree. A very special thanks is extended to Dr. Ralph Hutcheson, Dr. Randy Equall and everyone at Scientific Materials Corporation for their provision of sample laser materials and invaluable knowledge. I would also like to express thanks to the people who helped get this project started through the loaning of knowledge and equipment, namely, Dr. Patrik Callis and the Callis group, Dr. John Carlsten and the Carlsten group, Dr. Rufus Cone and the Cone group, Mr. Lee David, Mr. Dallas Johnston, Dr. Berk Knighton, Mr. Ray Larsen, Dr. Brian Metzger and Dr. David Singel and the Singel group. This project is completely a group effort and, therefore, I would like to thank my labmates Mr. Bruce Farris, Mr. Richard Hanson, Ms. Amy Hyfield, Mr. Anthony Smith and Ms. Wendi Sonnenberg. Without their efforts and perseverance success of this project could not be realized. And a final thanks goes to my parents for their caring and continual support.

TABLE OF CONTENTS

	Page
1. INTRODUCTION	1
General	1
Statement of the Problem	2
Spectroscopy of Rare-Earth Crystalline Laser Materials	3
The Chemistry and Physics of Laser Materials	4
Stark Level Employment in Operating Schemes	6
Dopant Ion Concentrations	7
Temperature Effects	8
Thulium Doped Materials	9
Co-Doped Materials	11
2. TIME-RESOLVED FOURIER TRANSFORM SPECTROSCOPY	15
Background	15
Step-Scan FTS Technique	16
Normalization of FT-TRS and Inherent Spectral Noise	20
TRSNomenclature	23
3. EXPERIMENTAL PROCEDURE	26
Sample Laser Materials	26
Experimental Apparatus	27
The Material Characterization Process	34
4. EXPERIMENTAL RESULTS	36
Absorption Spectra	36
Continuous Fluorescence Spectra	43
Time-Resolved Spectra	50
Excitation Via the 3H_4 Manifold	50
Tm ³⁺ :YAG	50
Tm ³⁺ :YALO	56
Tm ³⁺ :YSO	59
Tm ³⁺ :YO	62
Tm ³⁺ :LAG	63

TABLE OF CONTENTS - Continued

	Page
Excitation Via the 1G_4 Manifold	63
Tm^{3+} :YAG.....	63
Tm^{3+} :YALO.....	66
Excitation Via the 1D_2 Manifold	67
Tm^{3+} :YAG.....	69
Tm^{3+} :YALO.....	70
 5. DISCUSSION OF RESULTS	 75
General Experimental Results	75
Tm^{3+} :YAG.....	75
Tm^{3+} :YALO.....	77
Generation and Fitting of Experimental Decay Curves	78
Generation of Decay Curves	78
Mathematical Fits of Experimental Decay Curves	79
Kinetic Model of Experimental Data	85
Derivation of Rate Equations	85
Low Concentration Tm^{3+} :YAG.....	86
High Concentration Tm^{3+} :YAG	87
 6. CONCLUSIONS & SUMMARY	 93
Advantages and Limitations of FT-TRS	93
Closing Remarks.....	97
 REFERENCES CITED	 100

LIST OF TABLES

Table	Page
1. Experimental Lifetimes of Transitions in Tm^{3+} Doped Materials	72
2. 3F_4 Manifold Population (Rise) Times for Tm^{3+} Doped Materials	74
3. Values for Ionic Separation and C/C_0 Derived from the IH Fit	84
4. Summary of Terms Used for the Kinetic Model	89

LIST OF FIGURES

Figure	Page
1. The YAG crystal lattice	5
2. $2\mu\text{m}$ lasing operation scheme for $\text{Tm}^{3+}:\text{YAG}$	10
3. IR lasing operation scheme for $\text{CTH}:\text{YAG}$	12
4. Formation of the interferogram in rapid-scan mode vs. step-scan mode	18
5. Derivation of the time-resolved spectrum	19
6. Generation of systematic noise in FT-TRS spectra	21
7. Interferograms and corresponding spectra	22
8. A step-scan emission spectrum	24
9. Apparatus employed for absorption and emission studies	28
10. The Bruker IFS 66 step-scan interferometer	29
11. Spectra for detector/beamsplitter combinations	30
12. Spectra for KG3 and RG715 optical filters	33
13. IR (top) and visible absorption spectra for $\text{Tm}^{3+}:\text{YAG}$	38
14. IR (top) and visible absorption spectra for $\text{Tm}^{3+}:\text{LAG}$	39
15. IR (top) and visible absorption spectra for $\text{Tm}^{3+}:\text{YALO}$	40
16. IR (top) and visible absorption spectra for $\text{Tm}^{3+}:\text{YSO}$	41
17. IR (top) and visible absorption spectra for $\text{Tm}^{3+}:\text{YO}$	42

LIST OF FIGURES - Continued

	Page
18. IR (top) and visible continuous emission spectra for $\text{Tm}^{3+}:\text{YAG}$	45
19. IR (top) and visible continuous emission spectra for $\text{Tm}^{3+}:\text{LAG}$	46
20. IR (top) and visible continuous emission spectra for $\text{Tm}^{3+}:\text{YALO}$	47
21. IR (top) and visible continuous emission spectra for $\text{Tm}^{3+}:\text{YSO}$	48
22. IR (top) and visible continuous emission spectra for $\text{Tm}^{3+}:\text{YO}$	49
23. Time-resolved IR fluorescence spectrum for 0.25% $\text{Tm}^{3+}:\text{YAG}$. 400 μsec time resolution, 200 time slices, 10 co-adds	51
24. Decay of the ${}^3\text{F}_4 \rightarrow {}^3\text{H}_6$ transition for the 0.25% $\text{Tm}^{3+}:\text{YAG}$ sample	52
25. Time-resolved IR fluorescence spectrum for 0.25% $\text{Tm}^{3+}:\text{YAG}$. 20 μsec time resolution, 200 time slices and 20 co-adds	53
26. Decay of the ${}^3\text{H}_4 \rightarrow {}^3\text{F}_4$ transition at $6,800 \text{ cm}^{-1}$ for the 5 $\text{Tm}^{3+}:\text{YAG}$ samples.....	54
27. Log of intensity vs. time for the decay of ${}^3\text{H}_4 \rightarrow {}^3\text{F}_4$ transition at $6,800 \text{ cm}^{-1}$ for the 5 $\text{Tm}^{3+}:\text{YAG}$ samples	55
28. Population of the ${}^3\text{F}_4 \rightarrow {}^3\text{H}_6$ fundamental IR transition for the 5 $\text{Tm}^{3+}:\text{YAG}$ samples.....	56
29. Population of the ${}^3\text{H}_4 \rightarrow {}^3\text{F}_4$ transition at $6,800 \text{ cm}^{-1}$ for 0.25% $\text{Tm}^{3+}:\text{YAG}$	57
30. Time-resolved fluorescence spectrum for 0.1% $\text{Tm}^{3+}:\text{YALO}$. 250 μsec time resolution, 200 time slices, 10 co-adds	58
31. Decay of the ${}^3\text{F}_4 \rightarrow {}^3\text{H}_6$ transition for 0.1% $\text{Tm}^{3+}:\text{YALO}$	58
32. Log of intensity vs. time for the decay of the ${}^3\text{H}_4 \rightarrow {}^3\text{F}_4$ transition at $6,800 \text{ cm}^{-1}$ for the 2 $\text{Tm}^{3+}:\text{YALO}$ samples	59

LIST OF FIGURES - Continued

	Page
33. Population of the ${}^3F_4 \rightarrow {}^3H_6$ fundamental IR transition for the 2 Tm ³⁺ :YALO samples.....	60
34. Decay of the ${}^3F_4 \rightarrow {}^3H_6$ fundamental transition for Tm ³⁺ :YSO	61
35. Log of intensity versus time for the decay of the ${}^3H_4 \rightarrow {}^3F_4$ transition at 6,800 cm ⁻¹ for Tm ³⁺ :YSO	61
36. Decay of the ${}^3F_4 \rightarrow {}^3H_6$ fundamental transition for Tm ³⁺ :YO	62
37. Log of intensity versus time for the decay of the ${}^3H_4 \rightarrow {}^3F_4$ transition at 6,500 cm ⁻¹ for Tm ³⁺ :YO	63
38. Extracts at 20 μsec after red (upper) and blue excitation for 0.25% Tm ³⁺ :YAG.....	65
39. Trace integrations after blue excitation for 0.1% Tm ³⁺ :YALO	67
40. FT-TRS spectrum for 0.1% Tm ³⁺ :YALO for the 13,000 cm ⁻¹ region	68
41. Time-resolved visible (blue) fluorescence spectrum for 0.25% Tm ³⁺ :YAG. 5 μsec time resolution, 40 time slices and 20 co-adds	69
42. Log of intensity versus time for the decay of the ${}^1G_4 \rightarrow {}^3H_6$ transition at 22,000 cm ⁻¹ for the 3 Tm ³⁺ :YAG samples studied	70
43. Time-resolved visible (red) fluorescence spectrum for 0.25% Tm ³⁺ :YAG.....	71
44. Integration method employed to generate experimental trace decay curves.....	79
45. IH (solid line) fit to the ${}^3H_4 \rightarrow {}^3F_4$ non-exponential decay for 2.4% Tm ³⁺ :YAG.....	81
46. IH (solid line) fit to the ${}^3H_4 \rightarrow {}^3F_4$ non-exponential decay for 4.0% Tm ³⁺ :YAG.....	82

LIST OF FIGURES - Continued

	Page
47. IH (solid line) fit to the ${}^3\text{H}_4 \rightarrow {}^3\text{F}_4$ non-exponential decay for 5.2% $\text{Tm}^{3+}:\text{YAG}$	82
48. Ionic separation (\AA) versus C/C_0 derived from the IH fit	84
49. Energy level diagram for $\text{Tm}^{3+}:\text{YAG}$	86
50. Modeled decay (dashed) from manifold 3 (${}^3\text{H}_4$) vs. 0.25% experimental decay	88
51. Modeled decay (dashed) from manifold 1 (${}^3\text{F}_4$) vs. 0.25% experimental decay	88
52. Modeled decay (dashed) from manifold 3 (${}^3\text{H}_4$) vs. 2.4% experimental decay	90
53. Modeled decay (dashed) from manifold 3 (${}^3\text{H}_4$) vs. 4.0% experimental decay	91
54. Modeled decay (dashed) from manifold 3 (${}^3\text{H}_4$) vs. 5.2% experimental decay	91
55. Population of the $\text{Tm}^{3+} {}^3\text{H}_4$ (open circles) and $\text{Ho}^{3+} {}^5\text{I}_7$ manifolds after $12,800 \text{ cm}^{-1}$ excitation	94
56. FT-TRS spectrum for the population of the ${}^3\text{F}_4$ and ${}^5\text{I}_7$ manifolds of Tm^{3+} and Ho^{3+} , respectively in $\text{CTH}:\text{YAG}$	95

ABSTRACT

A new technique for the analysis of solid-state laser materials named Fourier Transform Time-Resolved Spectroscopy (FT-TRS) has been developed and implemented. FT-TRS has advantages over previous analysis techniques, primarily the time in which complete material characterization can be accomplished. The technique uses interferometric methods to collect sample emission after excitation over a broad spectral range while simultaneously characterizing the emission lifetime. In this way, analysis time is shortened considerably while providing information regarding absorption frequencies, emission frequencies and emission lifetimes which are essential for understanding the kinetics of the many photophysical processes which occur in these materials.

The interferometer used for our FT-TRS experiments can resolve spectral features to 0.25 cm^{-1} over a range of nearly $23,000 \text{ cm}^{-1}$ ($25,000\text{-}2,000 \text{ cm}^{-1}$). Temporal resolution to 20 nsec has been achieved. The implementation of an optically parametric oscillating laser enables material excitation from $23,000\text{-}5,500 \text{ cm}^{-1}$.

FT-TRS has been used for the analysis of several different thulium (Tm^{3+}) doped laser materials. The technique has proven to yield results consistent with earlier studies performed using different instrumentation. Emission rise and decay lifetimes for several electronic transitions have been determined. Mathematical fitting methods developed by Inokuti and Hirayama have proven to fit non-exponential emission decay that occurs in these materials. Subsequently, the kinetics which describe the many energy transfer events occurring after excitation have been investigated which has yielded the magnitudes of these radiative and non-radiative energy transfer processes.

CHAPTER 1

INTRODUCTION

General

Laser based analysis systems have been implemented in many areas of scientific research, as well as in monitoring applications and medicine. Examples include the study and identification of environmental pollutants through remote sensing (LIDAR), the determination of molecular orientation at a surface (SERS), the process of soft-ionization in laser desorption mass spectrometry (MALDI) and the development of surgical lasers. The creation of new laser technology and the improvement of laser designs currently in use is of paramount significance when considering the increasing complexity and importance of their roles in real world applications. As more demands are being made upon the scientific community to improve laser performance advances are also required in the analysis of the materials that serve as the lasing media.

Solid-state lasers are proving to be a practical source of light emission in the aforementioned areas of research. These lasers are very durable, are usually compact in size, quite powerful and generally can be operated at a variety of repetition rates. Coherent photon output in solid-state systems is dependent on the crystalline lasing

medium implemented. Laser performance is directly dependent on the optical properties of the lasing medium, such as emission. Spectroscopic analysis methods allow for a better understanding of the physical processes which occur in these crystalline materials. Based on the studies of these processes, materials may be evaluated and possibly improved.

Statement of the Problem

Currently, there are several hundred crystalline materials that have the potential for use in solid-state lasers. New materials may be developed at rapid rates, with crystal growth times generally on the order of a few days up to two weeks. Additionally, many growers have the capability of creating a variety of finished products in a single growing period. For example, Scientific Materials Corporation of Bozeman, MT created nearly fifty different materials in a two month span. Due to this ability to quickly manufacture materials and the limitations of current material analysis techniques it is the goal of this research to develop and apply a spectroscopic method that allows for rapid and accurate material characterization. Upon characterization, information may then be fed back to the grower to aid in their engineering processes or determine if the material is suitable for use in an operating laser system.

The method employed will allow for developing a better understanding of energy transfer processes which occur (radiative and nonradiative) after excitation. Spectroscopic results obtained via the new method will be compared to known and accepted data for validation of the method. In addition, a working kinetic model based

upon experimental results will be generated. During the initial studies of this project we hope to exploit the advantages of the technique while uncovering problems and limitations.

Spectroscopy of Rare-Earth Crystalline Laser Materials

The spectroscopic parameters of laser materials have been studied for over 30 years. Johnson, *et al.* in 1965 and 1966 studied emission from several different rare-earth ions doped into yttrium aluminum garnet ($Y_3Al_5O_{12}$ or YAG)(1).

Solid-state laser materials tend to have many absorption bands which are made up of relatively narrow line features. The materials absorb light over a broad wavelength region, but do so selectively due to the narrow line widths. In order to fully characterize a material it is beneficial to selectively excite the sample at many different energies and often at different sites within a particular absorption manifold. Upon excitation the material may then emit light. The emission is typically narrow band, but can occur over a broad wavelength region. Most spectroscopic emission data has been obtained by using either a laser or conventional source such as a tungsten or mercury lamp to excite the material. Emitting wavelengths from the material are typically dispersed using a monochromator and impinged on a photo-sensitive detector responsive to the wavelength(s) of interest. Emission lifetimes may be measured after pulsed excitation with the addition of an oscilloscope or a boxcar with sufficient temporal resolution capabilities. The determination of the emission lifetimes with a high degree of accuracy and precision is necessary to determine energy transfer rates. This method of analysis

is a very reliable and proven one, but is quite tedious and time-consuming.

The above characteristics of these materials shed light upon the requirements needed to effectively perform spectroscopic analyses. It is imperative that a narrow band source be employed that is tunable over a large frequency range (ultra-violet to near-infrared) to fully exploit the absorption features of the material. Recent laser developments (Optical Parametric Oscillation, OPO) have made this possible. Also, because many emissions occur within a nanosecond time frame, short output pulses are required. Since emission lifetimes can vary significantly for different processes (from milliseconds for emission from the first excited state to nanoseconds for inter-manifold transitions), variation of the laser output repetition rate is essential to allow for complete relaxation between pulses.

The device employed to detect and analyze emitting radiation must operate over a wide spectral range with sufficient resolution capabilities. In order to analyze data rapidly the system must simultaneously pass, detect and resolve as many emitting wavelengths as possible and the system must resolve the emission in 3 dimensions: intensity, wavelength and time. This is the major time limiting factor of previous analysis designs. We have found that the solution to the above requirements is the technique of step-scan interferometry and is outlined in Chapter 2.

The Chemistry and Physics of Laser Materials

The materials used in this study were grown by the Czochralski technique. The materials are conceived by starting with the compounds that will form the crystalline

lattice. It is imperative that these compounds be free of dopant or impurity ions, such as Nd^{3+} and OH^- , respectively. Typically, an iridium crucible is used to contain the "melt" which consists of the lattice precursors. The growing process is carried out at temperatures above 2200 degrees celcius. The dopant ion is introduced into the melt when it reaches the correct temperature for material formation. The crystal is then pulled slowly from the melt, for example, 0.6 mm/hr during Nd:YAG crystal formation(2). The temperature of the melt must be rigorously controlled by the grower to ensure that the dopant ion is distributed properly throughout the crystal as it is pulled. The dopant ion replaces a matrix ion (yttrium) at certain sites in YAG (see Figure 1), for example, which leads to a material that is capable of producing radiative emission that

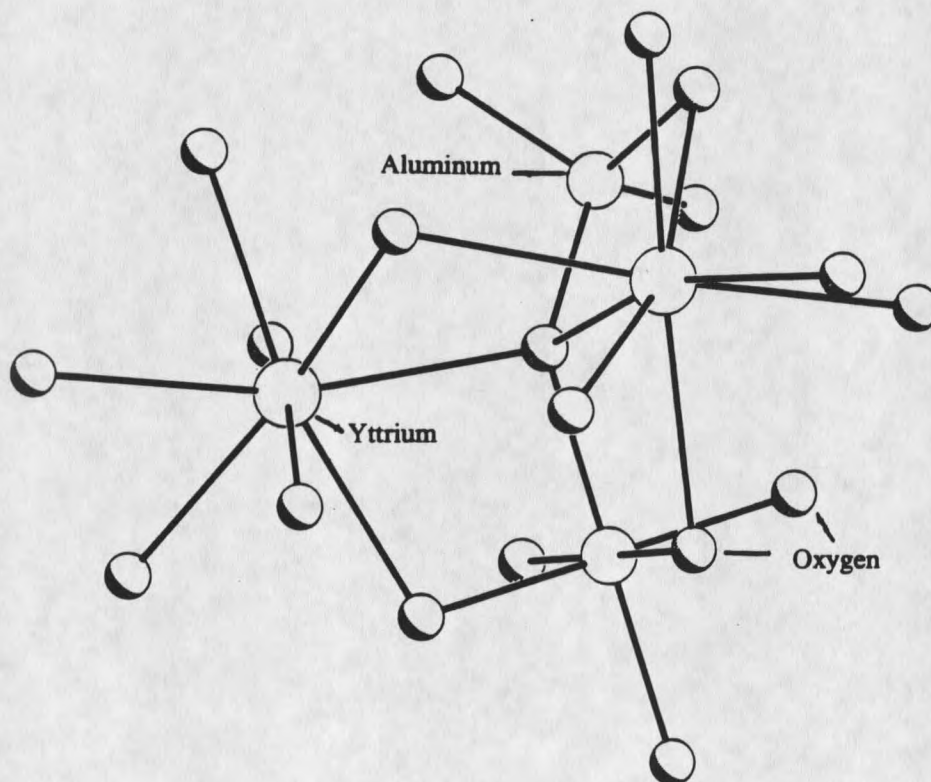


Figure 1. The YAG crystal lattice.

may be used for lasing under proper conditions(3). Again, it is important that the matrix and dopant materials be free of outside impurities such as the hydroxide ion. Hydroxide ion impurities with magnitudes of 1 to 4% in $\text{Nd}^{3+}:\text{YAG}$ have shown to cause a decrease of approximately 50% in lasing output power(4). This decrease is believed to be due to direct interaction of the Nd^{3+} ion with the OH^- impurity that resides in the dodecahedral site of the YAG lattice.

Stark Level Employment In Operating Schemes

It has been stated that the initial action to be taken when performing spectroscopic analyses of solid-state laser media is the identification and location of the characteristic absorption bands (Stark manifolds) and their corresponding features (Stark levels)(3). This process is most easily accomplished by light absorption methods. This determination allows for selective excitation, experimental emission energy transfer assignments and determination of other energy transfer processes such as upconversion and cross-relaxation, for example. While pre-existing calculated and experimental absorption data is a valuable resource, it is important to perform absorption measurements when samples are obtained for study, due to the possibility of changes in the optical properties caused by impurities.

Stark manifold location and level structure is governed by the electrostatic interaction of the 4f electrons with one another, the spin-orbit coupling of the electrons and the influence of the lattice crystal field.(5) The Coulombic interaction generates the $2s+1L$ terms which are generally separated by thousands of cm^{-1} . The spin-orbit coupling splits the total angular momentum J states. The influence of the crystal field

then splits the Stark manifolds into their fine structure (Stark levels) with a degeneracy equal to $2J+1$ (5). The strength of the crystal field interaction with the dopant ion determines the energy spacing of the Stark levels within a given manifold. Most often, materials grown using rare-earth metals with a +3 charge experience a weak interaction with the crystal field due to the inner 4f electrons being shielded from the surrounding environment (host lattice) by the outer 5s and 5p electrons.(3,5,6) Consequently, the energy spacing between Stark levels is small, typically on the order of $10-100 \text{ cm}^{-1}$. Often, many different lattice materials are grown with the same dopant ion. This is done so that small energy shifts of the Stark levels may be accomplished leading to a laser material that may be employed in a desired application.

The crystal field is also responsible for inducing oscillator strength into specific transitions. The magnitude of the oscillator strength reveals the probability of radiative energy transfer between given Stark levels.

Dopant Ion Concentrations

Spectroscopic analysis of emission from the material as dopant concentration is varied over a large gradient is required in order to investigate ion-ion interactions(3). An experiment performed by Zhekov, *et al.*(7), described the effects of varying the concentration of Er^{3+} ions doped into YAG. The authors found that the optimum amount of doped Er^{3+} was 15% when observing the IR fluorescence decay at approximately $6,000 \text{ cm}^{-1}$. At very low (0.5%) and very high (100%) amounts of Er^{3+} the experimental lifetime decreased dramatically from a maximum lifetime of 9 msec obtained at 6% Er^{3+} to 6.5 msec and 0.25 msec, respectively. These results were

confirmed by Shi, *et al.*(8) in a similar study. Similarly, Becker, *et al.*(9), as well as Armagan, *et al.*(10) showed that as the Tm^{3+} concentration in YAG was increased the lifetime of the experimental emission from the 3H_4 manifold near 780 nm to the 3H_6 ground state became significantly shorter.

When high dopant ion concentrations are used self-quenching becomes an issue of concern. Self-quenching, often called concentration quenching or cross-relaxation, is a non-radiative, resonant energy transfer that can depopulate the upper laser level and have a detrimental effect on the lasing process as in the case of Er^{3+} :YAG.(7,8) Self-quenching is due solely to dopant ion-dopant ion interactions. As the concentration of the dopant ion increases the ions become closer to each other spatially. It has been determined by Dexter, *et al.*(11), as well as, Inotaki and Hirayama(12), that this cross-relaxing quenching process is generally dominated by electric dipole-dipole interactions described by an R^{-6} distance dependence. The process may also be dependent on the energy of the exciting photons(8), as well as the temperature of the crystal.

Temperature Effects

Radiative and non-radiative emission lifetimes in Tm^{3+} doped laser materials are substantially affected by changes in temperature. Zverev, *et al.*(13), observed that for Tm^{3+} :YAG as temperature was increased from 77 to 900 degrees K the experimental emission lifetime of the $^3F_4 \rightarrow ^3H_6$ transition decreased from 8.5ms to 2.5ms. This effect was described as temperature quenching. The decrease in lifetime is due to an increase in the probability of stimulated nonradiative (vibronic) transitions that depopulate the upper-laser manifold of the material (3F_4)(14). In effect, as temperature increases, the

non-radiative processes (phonons, eg.) that occur within a sample begin to dominate the radiative processes. It is known that non-radiative decay events, as well as their reliance on variance in temperature are determined by the size of the dopant ion and its symmetry within a lattice(15). Therefore, for Tm^{3+} doped into different lattices, lifetimes may decrease over a temperature gradient with varying degrees of magnitude. It should be noted that a decrease in fundamental lifetime did not occur until the temperature reached approximately 475 K. A similar trend has been observed for lasing output power in three Tm^{3+} doped materials. As the crystal temperature was raised from 258 to 303 K the output power in Tm:YAG, Tm:YLAG and Tm:LAG decreased 8%, 7% and 11%, respectively(16).

Based on theoretical calculations, Riseberg and Weber(5) have shown that as temperature is increased from 0 to 400 degrees K, the rate of non-radiative multiphonon emission increases substantially and varies depending on the number of phonons involved in the emission. This supports the theory that as temperature is increased non-radiative decay becomes very significant and can have a detrimental effect on radiative energy transfer.

Thulium

Tm^{3+} has been used as an activator ion in laser materials for approximately 30 years(1,2) and is the main ion of focus in our studies. Tm^{3+} follows a quasi-four-level laser operating scheme with one metastable state when introduced as the dopant ion in YAG, where one Y^{3+} ion is replaced by one Tm^{3+} ion(3,17).

Most often, the ${}^3\text{H}_4$ Stark manifold near $12,800\text{ cm}^{-1}$ is pumped to initiate the energy transfer process where simultaneous radiative and non-radiative emissions occur from the ${}^3\text{H}_4$ manifold to the ${}^3\text{H}_5$ manifold. At sufficiently large Tm^{3+} concentrations, non-radiative energy decay to the ${}^3\text{F}_4$ manifold readily occurs(18). Non-radiative multiphonon emission dominates the energy decay from the ${}^3\text{H}_5$ to the ${}^3\text{F}_4$ manifold because of the small energy gap ($2,000\text{ cm}^{-1}$). This is followed by a long-lived radiatively dominated emission to the ${}^3\text{H}_6$ ground state (see Figure 2). These emission

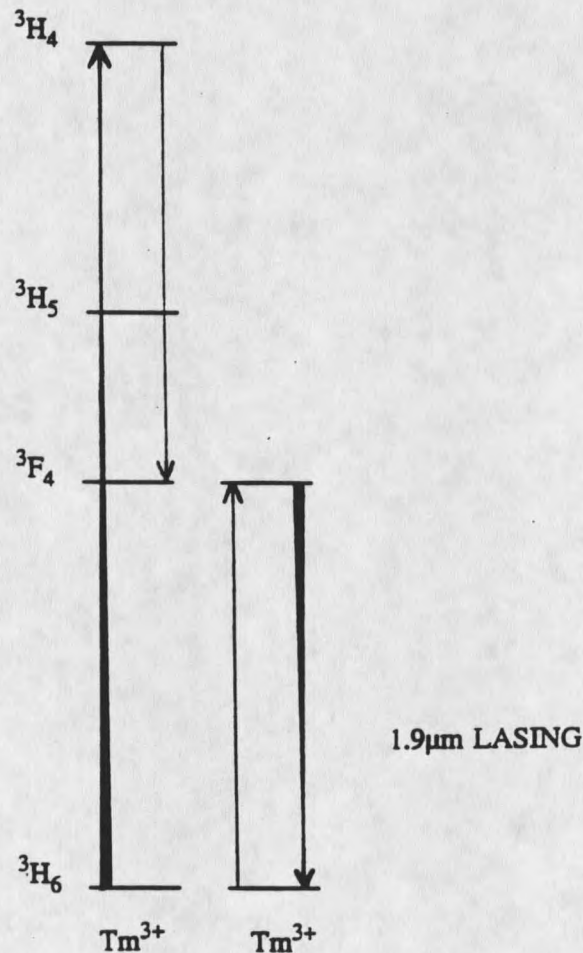


Figure 2. $2\mu\text{m}$ lasing operation scheme for $\text{Tm}^{3+}:\text{YAG}$.

processes have been studied previously(1,9,18,20,21).

An additional and very important photophysical process that occurs in $\text{Tm}^{3+}:\text{YAG}$ is also shown in Figure 2. This is the cross-relaxation process which occurs due to the resonance caused by the energy gap between the ${}^3\text{F}_4\text{-}{}^3\text{H}_4$ and ${}^3\text{F}_4\text{-}{}^3\text{H}_6$ manifolds. At large enough dopant-ion concentrations the emission from the ${}^3\text{H}_4$ to the ${}^3\text{F}_4$ manifold of one Tm^{3+} is quenched by a neighboring Tm^{3+} within the lattice due to their proximity to one another(19). The cross-relaxation is not detrimental to the fundamental lasing transition because it aids in the population of the ${}^3\text{F}_4$ upper-laser manifold. This process is responsible for nearly doubling the pump quantum efficiency(20) and is important because losses in radiative emission from the ${}^3\text{F}_4$ manifold due to temperature increases within the sample can be avoided(9). The fundamental transition (${}^3\text{F}_4 \rightarrow {}^3\text{H}_6$) in Tm^{3+} is of particular importance because water has absorption bands at this wavelength. A laser operating at this wavelength may be applied in studies of the environment, body tissues and remote sensing (LIDAR)(21).

Co-Doped Materials

Tm^{3+} may be introduced into various lattices with co-dopant ions such as Cr^{3+} , Ho^{3+} and Er^{3+} with varying concentrations. Early studies by Johnson, *et al.*(1) have shown how co-dopant strategies can enhance laser performance. The IR emission from the ${}^3\text{F}_4$ manifold to the ground state near $5,200 \text{ cm}^{-1}$ in 1 atomic % $\text{Tm}^{3+}:\text{YAG}$ was enhanced by a factor of 40 by replacing 50% of the yttrium ions in the YAG matrix with erbium ions.

Most often, when Tm^{3+} is used in a co-doped laser material, its role is to serve

